

Genome-wide meta-analyses of multiancestry cohorts identify multiple new susceptibility loci for refractive error and myopia

Refractive error is the most common eye disorder worldwide and is a prominent cause of blindness. Myopia affects over 30% of Western populations and up to 80% of Asians. The CREAM consortium conducted genome-wide meta-analyses, including 37,382 individuals from 27 studies of European ancestry and 8,376 from 5 Asian cohorts. We identified 16 new loci for refractive error in individuals of European ancestry, of which 8 were shared with Asians. Combined analysis identified 8 additional associated loci. The new loci include candidate genes with functions in neurotransmission (*GRIA4*), ion transport (*KCNQ5*), retinoic acid metabolism (*RDH5*), extracellular matrix remodeling (*LAMA2* and *BMP2*) and eye development (*SIX6* and *PRSS56*). We also confirmed previously reported associations with *GJD2* and *RASGRF1*. Risk score analysis using associated SNPs showed a tenfold increased risk of myopia for individuals carrying the highest genetic load. Our results, based on a large meta-analysis across independent multiancestry studies, considerably advance understanding of the mechanisms involved in refractive error and myopia.

Refractive error is the leading cause of visual impairment in the world¹. Myopia, or nearsightedness, in particular is associated with structural changes of the eye, increasing the risk of severe complications, such as macular degeneration, retinal detachment and glaucoma. The prevalence of myopia has been rising considerably over the past few decades², and it is estimated that 2.5 billion people will be affected by myopia within a decade³. Although several genetic loci influencing refractive error have been identified^{4–10}, their contribution to phenotypic variance is small, and many more loci are expected to explain its genetic architecture.

Here, the Consortium for Refractive Error and Myopia (CREAM) presents results from the largest international genome-wide meta-analysis on refractive error, with data from 32 studies from Europe, the United States, Australia and Asia. The meta-analysis was performed in 3 stages. In the first stage, we investigated the genome-wide association study (GWAS) results of 37,382 individuals

from 27 populations of European ancestry (Supplementary Table 1 and Supplementary Note) using spherical equivalent as a continuous outcome. In the second stage, we aimed to test the cross-ancestry transferability of the statistically significant associations from the first stage in 8,376 individuals from 5 Asian cohorts (Supplementary Table 1 and Supplementary Note). In the third stage, we performed a GWAS meta-analysis on the combined populations (total $n = 45,758$). Subsequently, we examined the influence of associated alleles on the risk of myopia in a genetic risk score analysis, and, lastly, we evaluated gene expression in ocular tissues and explored potential mechanisms by which newly found loci might exert their effects on refractive development.

In stage 1, we analyzed ~2.5 million autosomal SNPs for which data were obtained through whole-genome imputation of genotypes to HapMap 2. The inflation factors (λ_{GC}) of the test statistics in individual studies contributing to the meta-analysis ranged between 0.992 and 1.050, indicating excellent within-study control of population substructure (Supplementary Table 2). Overall λ was 1.09, consistent with a polygenic inheritance model for refractive error (quantile-quantile plot; Supplementary Fig. 1). We did not perform a correction for λ , as it has been shown that, under polygenic inheritance, substantial genomic inflation can be expected, even in the absence of population structure and technical artifacts¹¹. We identified 309 SNPs that exceeded the conventional genome-wide significance threshold of $P = 5.0 \times 10^{-8}$ in the European ancestry sample. These SNPs were

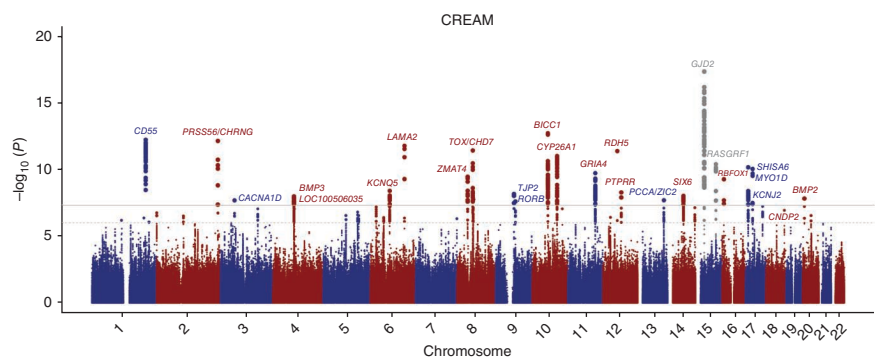


Figure 1 Manhattan plot of the GWAS meta-analysis for refractive error in the combined analysis ($n = 45,758$). The plot shows $-\log_{10}$ -transformed P values for all SNPs. The upper horizontal line represents the genome-wide significance threshold of $P < 5.0 \times 10^{-8}$; the lower line indicates P value of 1×10^{-5} . Previously reported genes are shown in gray. The *RBFOX1* gene is also known as *A2BP1*.

A full list of authors and affiliations appears at the end of the paper.

Received 3 October 2012; accepted 16 January 2013; published online 10 February 2013; doi:10.1038/ng.2554

Table 1 Genome-wide significant associations with refractive error in the European ancestry population with results in the Asian population and combined analysis

Locus number	SNP	Chromosome	Position	Nearest gene	Stage 1 (n = 37,382)		Stage 2 (n = 8,376)		Combined (n = 45,758)		P value	Heterogeneity					
					MAF	β	SE	P value	MAF	β			SE	P value			
1	rs1652333	1	203858855	CD55	G/A	0.32	-0.115	0.018	6.29 × 10 ⁻¹¹	0.42	-0.099	0.035	5.00 × 10 ⁻³	0.112	0.016	3.05 × 10 ⁻¹²	0.94
2	rs1656404	2	233205446	PRSS56	A/G	0.21	-0.151	0.025	2.38 × 10 ⁻⁹	0.11	-0.167	0.069	1.60 × 10 ⁻²	-0.153	0.024	7.86 × 10 ⁻¹¹	0.83
3	rs1881492	2	233406997	CHRNA1	T/G	0.22	-0.145	0.022	1.28 × 10 ⁻¹⁰	0.15	-0.057	0.110	6.09 × 10 ⁻¹	-0.139	0.021	5.15 × 10 ⁻¹¹	0.88
4	rs14165	3	53847407	CACNA1D	A/G	0.32	0.095	0.017	4.36 × 10 ⁻⁸	0.12	0.120	0.100	2.29 × 10 ⁻¹	0.096	0.017	2.14 × 10 ⁻⁸	0.25
5	rs1960445	4	81930813	BMP3	C/T	0.17	-0.147	0.026	1.19 × 10 ⁻⁸	0.11	0.034	0.055	5.32 × 10 ⁻¹	-0.114	0.024	1.25 × 10 ⁻⁶	0.31
6	rs12206363	6	129834628	LAMA2	C/T	0.10	0.228	0.034	1.13 × 10 ⁻¹¹	0.02	0.553	0.236	1.92 × 10 ⁻²	0.235	0.033	1.79 × 10 ⁻¹²	0.93
7	rs4237036	8	61701056	CHD7	C/T	0.35	0.097	0.017	1.52 × 10 ⁻⁸	0.23	0.043	0.040	2.81 × 10 ⁻¹	0.089	0.016	1.82 × 10 ⁻⁸	0.76
8	rs7837791	8	60179085	TOX	T/G	0.49	0.106	0.017	9.22 × 10 ⁻¹⁰	0.39	0.103	0.035	4.00 × 10 ⁻³	0.106	0.015	3.99 × 10 ⁻¹²	0.70
9	rs7829127	8	40726393	ZMAT4	G/A	0.25	0.116	0.020	3.04 × 10 ⁻⁹	0.11	0.112	0.055	4.23 × 10 ⁻²	0.116	0.018	3.69 × 10 ⁻¹⁰	0.66
10	rs7042950	9	77149836	ROXB	G/A	0.24	-0.113	0.020	1.02 × 10 ⁻⁸	0.42	-0.040	0.037	2.72 × 10 ⁻¹	-0.096	0.018	4.15 × 10 ⁻⁸	0.83
11	rs10882165	9	94924323	CYP26A1	T/A	0.42	-0.111	0.016	1.25 × 10 ⁻¹¹	0.20	-0.060	0.056	2.84 × 10 ⁻¹	-0.107	0.016	1.03 × 10 ⁻¹¹	0.90
12	rs7084402	10	60265403	BICC1	G/A	0.48	-0.111	0.016	7.23 × 10 ⁻¹²	0.50	-0.094	0.035	7.34 × 10 ⁻³	-0.108	0.015	2.06 × 10 ⁻¹³	0.71
13	rs11601239	11	105061808	GRIN4	C/G	0.46	-0.092	0.017	3.45 × 10 ⁻⁸	0.42	-0.129	0.058	2.70 × 10 ⁻²	-0.095	0.016	5.92 × 10 ⁻⁹	0.83
14	rs3138144	12	56114768	RDH5	C/G	0.48	0.113	0.018	4.28 × 10 ⁻¹⁰	0.45	0.157	0.072	3.00 × 10 ⁻²	0.119	0.017	4.44 × 10 ⁻¹²	0.09
15	rs2184971	13	100818091	PCGA	G/A	0.44	0.095	0.016	5.90 × 10 ⁻⁹	0.22	0.022	0.040	5.84 × 10 ⁻¹	0.085	0.015	2.11 × 10 ⁻⁸	0.96
16	rs8000973	13	100691366	ZIC2	T/C	0.47	0.089	0.016	4.24 × 10 ⁻⁸	0.22	0.030	0.041	4.63 × 10 ⁻¹	0.081	0.015	5.10 × 10 ⁻⁸	0.50
17	rs524952	15	35005885	GJD2 ^a	A/T	0.48	-0.154	0.021	1.11 × 10 ⁻¹³	0.44	-0.193	0.060	1.00 × 10 ⁻³	-0.158	0.020	1.44 × 10 ⁻¹⁵	0.22
18	rs4778879	15	79372874	RASGRF1 ^a	G/A	0.44	-0.103	0.017	1.27 × 10 ⁻⁹	0.39	-0.103	0.043	1.50 × 10 ⁻²	-0.102	0.015	4.25 × 10 ⁻¹¹	0.15
19	rs17183295	17	31078271	MYO1D	T/C	0.23	-0.132	0.021	3.04 × 10 ⁻¹⁰	0.16	-0.166	0.144	2.49 × 10 ⁻¹	-0.131	0.020	9.66 × 10 ⁻¹¹	0.34
20	rs4793501	17	68718733	KCNJ2	G/A	0.42	0.096	0.016	3.21 × 10 ⁻⁹	0.44	0.010	0.034	7.64 × 10 ⁻¹	0.080	0.014	2.79 × 10 ⁻⁸	0.04
21	rs12971120	18	72174022	CNDP2	C/T	0.23	0.108	0.020	4.39 × 10 ⁻⁸	0.30	0.014	0.063	8.27 × 10 ⁻¹	0.099	0.019	1.85 × 10 ⁻⁷	0.49

Summary of SNPs that showed genome-wide significant ($P < 5 \times 10^{-8}$) association with spherical equivalent (SE) in subjects of European ancestry (stage 1), with results of replication in Asians (stage 2) and combined analysis (stage 3). We tested for heterogeneous effects between the Asian and European ancestry samples, for which P values are shown. Nearest gene, reference NCBI build 37; A1, reference allele; A2, other allele; MAF, average minor allele frequency; β, effect size on spherical equivalent in diopters based on allele A1.

^aPreviously reported genes.

clustered in 18 distinct genomic regions across 14 chromosomes (Fig. 1 and Table 1). In stage 2, we investigated the 18 best-associated SNPs in the Asian population: 10 showed evidence of association (Table 1). The most significant association in both ancestry groups was at a previously identified locus on chromosome 15q14 in the proximity of the *GJD2* gene (encoding the connexin 36 gap-junction protein; rs524952; $P_{\text{combined}} = 1.44 \times 10^{-15}$)^{4,12}. The locus near the *RASGRF1* gene (encoding Ras protein-specific guanine nucleotide-releasing factor 1) was also replicated in the meta-analysis (rs4778879; $P_{\text{combined}} = 4.25 \times 10^{-11}$)⁹. The remaining 16 loci associated at genome-wide significance had not previously been reported in association with refractive error. Those loci that did not show significant association in the smaller sized Asian population mostly had a similar effect size and direction of effect as in the European ancestry sample. In stage 3, we identified eight additional loci with associations that exceeded genome-wide significance in the combined analysis (Table 2). Regional and forest plots of the associated loci are provided in Supplementary Figures 2 and 3, respectively.

Genotype distributions of the risk alleles were evaluated in Rotterdam Studies 1–3 ($n = 9,307$). The clinical usefulness for the prediction of risk of myopia was evaluated by a weighted genetic risk score analysis based on the aggregate of effects (β regression coefficients) of individual SNPs derived from the meta-analysis, using the middle risk category as a reference. Risk scores ranged from a mean risk score of 1.88 (95% confidence interval (CI) = 1.86–1.89) in the lowest risk score category to 3.63 (95% CI = 3.61–3.65) in the highest risk score category. Having the lowest or the highest genetic risk score was associated with an odds ratio (OR) of 0.38 (95% CI = 0.18–0.77) and an OR of 10.97 (95% CI = 3.73–31.25) of myopia, respectively (Fig. 2). The predictive value (area under the receiver operating characteristic curve, AUC) of myopia versus hyperopia was 0.67 (95% CI = 0.65–0.69), a relatively high value for genetic factors in a complex trait^{13,14}. The genetic variants explained 3.4% of the phenotypic variation in refractive error in the Rotterdam Study.

We examined the expression of genes harboring a genetic association signal by measuring the levels of RNA in various eye tissues and found most of these genes expressed in the eye (Supplementary Table 3). Expression data for the *PRSS56*, *LOC100506035* and *SHISA6* genes were not available; all other genes were expressed in the retina. Subsequently, we assessed the areas with associated SNPs for acetylation at histone H3 lysine 27 (H3K27ac) modifications¹⁵ and HaploReg¹⁶ annotations for marks of active regulatory elements (Supplementary Fig. 4 and Supplementary Table 4). We found that many associated loci contained these elements, and alteration of regulatory function is therefore a potential mechanism.

The widely accepted model for myopia development is that eye growth is triggered by a visually evoked signaling cascade, which originates from the sensory retina, traverses the retinal pigment epithelium (RPE) and choroid and terminates in the sclera, where active extracellular matrix (ECM) remodeling results in a relative elongation of the eye¹⁷. Many of the genes in or near the identified loci can be linked to biological processes that drive this cascade. Neurotransmission in the retina is a necessary mechanism for eye growth regulation; the most significantly associated gene *GJD2* has a role in this process. This gene forms a gap junction between neuronal cells in the retina, enabling the intercellular exchange of small molecules and ions. The other previously reported gene *RASGRF1* is a nuclear exchange factor that promotes the exchange of GTP for GDP on Ras family GTPases and is involved in the synaptic transmission of photoreceptor responses^{18,19}. Both *GJD2* and *RASGRF1* knockout mice show retinal photoreception defects^{18,20}. One of the newly

Table 2 Additional genome-wide significant associations from the combined meta-analysis ($n = 45,758$)

Locus number	SNP	Chromosome	Position	Nearest gene	A1/A2	β	SE	P value	MAF	β	SE	P value	MAF	β	SE	P value	P value
						Combined ($n = 45,758$)				Stage 1 ($n = 37,382$)				Stage 2 ($n = 8,376$)			
1	rs9307551	4	80530670	<i>LOC100506035</i>	A/C	-0.099	0.017	1.09×10^{-8}	0.25	-0.097	0.020	1.37×10^{-6}	0.50	-0.105	0.035	3.06×10^{-3}	0.70
2	rs7744813	6	73643288	<i>KCNQ5</i>	C/A	0.112	0.019	4.18×10^{-9}	0.41	0.114	0.021	6.80×10^{-8}	0.33	0.094	0.046	4.30×10^{-2}	0.14
3	rs11145465	9	71766592	<i>TJP2</i>	A/C	-0.124	0.021	7.26×10^{-9}	0.25	-0.125	0.023	6.92×10^{-8}	0.07	-0.136	0.091	1.35×10^{-1}	0.14
4	rs12229663	12	71249995	<i>PTPRR</i>	G/A	0.099	0.017	5.47×10^{-9}	0.27	0.104	0.019	5.46×10^{-8}	0.36	0.080	0.052	1.23×10^{-1}	0.74
5	rs1254319	14	60903756	<i>SIX6</i>	A/G	-0.088	0.015	1.00×10^{-8}	0.32	-0.088	0.017	2.03×10^{-7}	0.34	-0.087	0.036	1.57×10^{-2}	0.59
6	rs17648524	16	7459682	<i>RBFOX1</i>	C/G	-0.118	0.019	5.64×10^{-10}	0.36	-0.116	0.022	7.48×10^{-8}	0.14	-0.140	0.058	1.60×10^{-2}	0.24
7	rs2969180	17	11407900	<i>SHISA6</i>	A/G	-0.101	0.015	7.29×10^{-11}	0.36	-0.101	0.019	7.51×10^{-8}	0.45	-0.097	0.034	4.00×10^{-3}	0.41
8	rs235770	20	6761764	<i>BMP2</i>	T/C	-0.089	0.016	1.57×10^{-8}	0.39	-0.088	0.017	1.34×10^{-7}	0.33	-0.087	0.050	8.20×10^{-2}	0.78

Summary of SNPs that showed genome-wide significant ($P < 5 \times 10^{-8}$) association with spherical equivalent in the combined analysis (stage 3), with results in subjects of European ancestry (stage 1) and Asians (stage 2). We tested for heterogeneous effects between the two ancestry groups, for which P values are shown. Nearest gene, reference NCBI build 37. The *RBFOX1* gene is also known as *A2BP1*.

identified genes, *GRIA4* (encoding glutamate receptor, ionotropic, AMPA 4; rs11601239; $P_{\text{combined}} = 5.92 \times 10^{-9}$), also has a potential function in this pathway. This gene encodes a glutamate-gated ion channel that mediates fast synaptic excitatory neurotransmission²¹, is present in various retinal cells²² and has been shown to be critical for light signaling in the retina²³ and emmetropization²⁴. Another gene involved in synaptic transmission is *RBFOX1* (encoding RNA-binding protein, fox-1 homolog; also known as *A2BP1*; rs17648524; $P_{\text{combined}} = 5.64 \times 10^{-10}$), encoding an RNA-binding splicing regulator that modulates membrane excitability²⁵.

We identified for the first time a number of candidate genes involved in ion transport, channel activity and the maintenance of membrane potential. *KCNQ5* (encoding a member of the potassium voltage-gated channel KQT-like subfamily; rs7744813; $P_{\text{combined}} = 4.18 \times 10^{-9}$), participates in the transport of potassium ions from the retina to the choroid and may contribute to voltage-gated potassium ion channels in the photoreceptors and retinal neurons associated with myopia^{26,27}. *CD55* (encoding a decay-accelerating factor for complement; rs1652333; $P_{\text{combined}} = 3.05 \times 10^{-12}$) is known to elevate cytosolic calcium ion concentration. Other ion channel genes that were associated include *CACNA1D* (encoding a voltage-sensitive calcium channel regulator; rs14165; $P_{\text{combined}} = 2.14 \times 10^{-8}$), *KCNJ2* (encoding a regulator of potassium ion transport; rs4793501; $P_{\text{combined}} =$

2.79×10^{-8}), *CHRNA3* (encoding a nicotinic cholinergic receptor; rs1881492; $P_{\text{combined}} = 2.15 \times 10^{-11}$) and *MYO1D* (encoding a putative binder of calmodulin; rs17183295; $P_{\text{combined}} = 9.66 \times 10^{-11}$), which mediates calcium ion sensitivity to *KCNQ5* ion channels.

Retinoic acid is synthesized in the retina, is highly expressed in the choroid and has been implicated in eye growth in experimental myopia models²⁸⁻³⁰. *RDH5* (encoding retinol dehydrogenase 5; rs3138144; $P_{\text{combined}} = 4.44 \times 10^{-12}$), a new refractive error susceptibility gene is involved in the recycling of 11-*cis*-retinal in the visual cycle³¹. Mutations in *RDH5* cause congenital stationary night blindness (MIM 136880), a disease associated with myopia. Other genes involved in retinoic acid metabolism are *RORB* (encoding RAR-related orphan receptor; rs7042950; $P_{\text{combined}} = 4.15 \times 10^{-8}$) and *CYP26A1* (encoding a member of the cytochrome P450 superfamily; rs10882165; $P_{\text{combined}} = 1.03 \times 10^{-11}$), genes that showed significant associations in the European ancestry studies. Notably, retinoic acid contributes to ECM remodeling by regulating cell differentiation.

ECM remodeling of the sclera is the pathological hallmark of myopia development. *LAMA2* (encoding laminin $\alpha 2$; rs12205363; $P_{\text{combined}} = 1.79 \times 10^{-12}$) is the most prominent gene in this respect. The *LAMA2* protein forms a subunit of the heterotrimer laminins, which are essential components of basement membranes, stabilizing cellular structures and facilitating cell migration³². Two genes encoding bone morphogenetic proteins (*BMP2*: rs235770; $P_{\text{combined}} = 1.57 \times 10^{-8}$ and *BMP3*: rs1960445; $P_{\text{stage 1}} = 1.19 \times 10^{-8}$; $P_{\text{combined}} = 1.25 \times 10^{-6}$) also have a role in the ECM architecture. They are members of the transforming growth factor (TGF)- β superfamily, regulate the growth and differentiation of mesenchymal cells and may orchestrate the organization of other connective tissues than bone, such as sclera. Notably, *BMP2* shows expression in RPE in animal models of myopia³³.

Genes involved in eye development appeared as a separate entity among the gene functions. *SIX6* (encoding SIX homeobox 6; rs1254319; $P_{\text{combined}} = 1.00 \times 10^{-8}$) has been linked to anophthalmia and glaucoma^{34,35}, *PRSS56* (encoding protease serine 56, rs1656404; $P_{\text{combined}} = 7.86 \times 10^{-11}$) has been linked to microphthalmia³⁶⁻³⁸, *CHD7* (encoding chromodomain helicase DNA-binding protein 7; rs4237036; $P_{\text{combined}} = 1.82 \times 10^{-8}$) has been linked to CHARGE syndrome, a congenital condition with severe eye structural defects, and *ZIC2* (encoding a member of the ZIC family of C2H2-type zinc-finger proteins; rs8000973; $P_{\text{combined}} = 5.10 \times 10^{-8}$) has been linked to brain development, including visual perception. For the remaining new associated loci, a mechanism in the pathogenesis of myopia is not immediately clear. Results from Ingenuity and the Protein Link Evaluator³⁹ (Supplementary Fig. 5) map the subcellular location of all associated gene products and show their inter-relationships. Direct connections between genes were infrequent, suggesting molecular

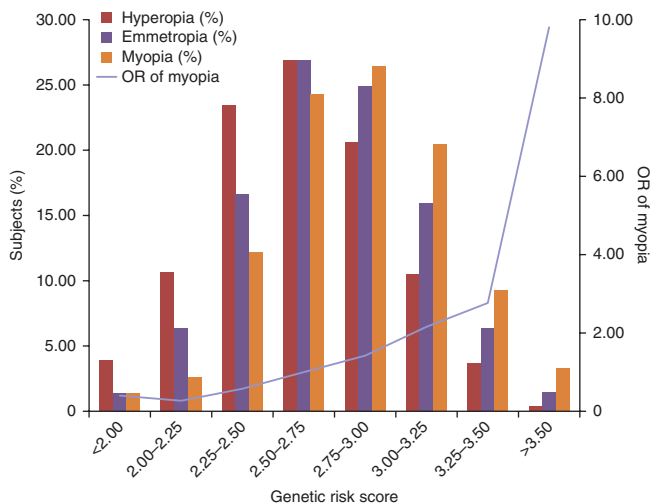


Figure 2 Genetic risk score for myopia. Distribution of subjects from Rotterdam Study 1-3 ($n = 9,307$) with myopia ($SE \leq -3$ diopters (D)), emmetropia ($SE \geq -1.5$ D and ≤ 1.5 D) and hyperopia ($SE \geq 3$ D) as a function of the genetic risk score. This score is based on the regression coefficients and allele dosages of the associated SNPs for all 26 loci identified in the meta-analysis. Mean OR of myopia was calculated per risk category, using the middle risk score category (risk score of 2.50-2.75) as a reference.

disease heterogeneity or functional redundancy in the pathobiological events involved in the development of refractive error and myopia.

In summary, we identified 24 new loci associated with refractive error through a large-scale meta-analysis of GWAS from international multiethnicity studies. The substantial overlap in genetic loci for refractive error between individuals of European ancestry and Asians provides evidence for shared genetic risk factors between the populations. The tenfold increased risk of myopia for those carrying the highest number of risk alleles shows the clinical significance of our findings. Further elucidation of the mechanisms by which these loci affect eye growth carries the potential to improve the visual outcome of this common trait.

URLs. R, <http://www.r-project.org/>; LocusZoom, <http://csg.sph.umich.edu/locuszoom/>; Ingenuity, <http://www.ingenuity.com/>.

METHODS

Methods and any associated references are available in the [online version of the paper](#).

Accession codes. Data on RPE gene expression have been deposited at the Gene Expression Omnibus (GEO) under accession [GSE20191](#).

Note: Supplementary information is available in the [online version of the paper](#).

ACKNOWLEDGMENTS

We gratefully thank the invaluable contributions of all study participants, their relatives and staff at the recruitment centers. Complete funding information and acknowledgments by study can be found in the **Supplementary Note**.

AUTHOR CONTRIBUTIONS

V.J.M.V., P.G.H., R.W., C.J.H., C.C.W.K., A.W.H., D.A.M., T.L.Y. and C.M.v.D. performed analyses and drafted the manuscript. C.C.W.K., D.S., C.J.H., J.E.B.-W., S.-M.S., C.M.v.D., A.H., D.A.M., S.M., A.D.P., V.V., C.W., P.N.B., T.-Y.W., J.S.R., T.L.Y., K.O., O. Pärssinen, S.P.Y., J.A.G., A. Metspalu, M.P., S.K.I. and N.P. jointly conceived the project and supervised the work. J.E.B.W., S.-M.S., D.A.M., T.L.Y., C.J.H., C.C.W.K., D.S., J.E.B.-W., C.M.v.D., R.W., P.G.H., V.J.M.V., K.O., Y.-Y.T., T.-Y.W., P.N.B., V.V., N.A., B.A.O., A.H., J.R.V., F.R., A.G.U., N.P., C.M., A. Mirshahi, T.Z., B.F., J.F.W., Z.V., O. Polasek, A.F.W., C.H., I.R., S.K.I., E.C., J.H.L., R.P.I., S.J., M.S., J.J.W., P.M., I.C., J.S.R., P.M.C., C.E.P., G.W.M., A. Mishra, W.A., F.M., M.P., L.C.K., T.D.S., E.Y.-D., A.N., O.R., C.-C.K., T.M., A.D., R.T.O., Y.Z., J.L., R.L., P.C., V.A.B., W.-T.T., E.V., T.A., E.-S.T., A. Metspalu, T.H., R.K., B.E.K.K., J.E.C., K.P.B., L.J.C., C.P.P., D.W.H.H., S.P.Y., J.W., O. Pärssinen, J.B.J., L.X., H.S.W., S.M.H., A.D.P., M.K., T.L., K.-M.M., C.L.S., C.W., N.J.T., D.M.E., B.S.P., J.P.K., G.M., G.H.S.B., M.K.I., X.Z., C.-Y.C., A.W.H., S.M., R.H., J.A.G. and Q.F. were responsible for study-specific data. G.H.S.B., V.J.M.V., Q.F. and J.A.G. were involved in the genetic risk score analysis. T.L.Y., A.A.B.B., T.G.M.F.G. and F.H. performed the data expression experiments. A.A.B.B., T.G.M.F.G., A.M. and S.M. were involved in pathway analyses. J.E.B.-W., S.-M.S., D.A.M., T.L.Y., K.O., T.-Y.W., P.N.B., T.G.M.F.G., S.K.I., E.C., J.J.W., A.J.M.H.V., C.-C.K., B.E.K.K., S.P.Y., C.W., N.J.T., G.H.S.B., M.K.I., A.W.H. and J.A.G. critically reviewed the manuscript.

COMPETING FINANCIAL INTERESTS

The authors declare no competing financial interests.

Published online at <http://www.nature.com/doi/10.1038/ng.2554>.

Reprints and permissions information is available online at <http://www.nature.com/reprints/index.html>.

1. Wojciechowski, R. Nature and nurture: the complex genetics of myopia and refractive error. *Clin. Genet.* **79**, 301–320 (2011).
2. Mutti, D.O. *et al.* Axial growth and changes in lenticular and corneal power during emmetropization in infants. *Invest. Ophthalmol. Vis. Sci.* **46**, 3074–3080 (2005).
3. Smith, T.S., Frick, K.D., Holden, B.A., Fricke, T.R. & Naidoo, K.S. Potential lost productivity resulting from the global burden of uncorrected refractive error. *Bull. World Health Organ.* **87**, 431–437 (2009).
4. Solouki, A.M. *et al.* A genome-wide association study identifies a susceptibility locus for refractive errors and myopia at 15q14. *Nat. Genet.* **42**, 897–901 (2010).
5. Shi, Y. *et al.* Genetic variants at 13q12.12 are associated with high myopia in the Han Chinese population. *Am. J. Hum. Genet.* **88**, 805–813 (2011).

6. Nakanishi, H. *et al.* A genome-wide association analysis identified a novel susceptible locus for pathological myopia at 11q24.1. *PLoS Genet.* **5**, e1000660 (2009).
7. Li, Z. *et al.* A genome-wide association study reveals association between common variants in an intergenic region of 4q25 and high-grade myopia in the Chinese Han population. *Hum. Mol. Genet.* **20**, 2861–2868 (2011).
8. Li, Y.J. *et al.* Genome-wide association studies reveal genetic variants in *CTNND2* for high myopia in Singapore Chinese. *Ophthalmology* **118**, 368–375 (2011).
9. Hysi, P.G. *et al.* A genome-wide association study for myopia and refractive error identifies a susceptibility locus at 15q25. *Nat. Genet.* **42**, 902–905 (2010).
10. Fan, Q. *et al.* Genetic variants on chromosome 1q41 influence ocular axial length and high myopia. *PLoS Genet.* **8**, e1002753 (2012).
11. Yang, J. *et al.* Genomic inflation factors under polygenic inheritance. *Eur. J. Hum. Genet.* **19**, 807–812 (2011).
12. Verhoeven, V.J. *et al.* Large scale international replication and meta-analysis study confirms association of the 15q14 locus with myopia. The CREAM consortium. *Hum. Genet.* **131**, 1467–1480 (2012).
13. Speliotes, E.K. *et al.* Association analyses of 249,796 individuals reveal 18 new loci associated with body mass index. *Nat. Genet.* **42**, 937–948 (2010).
14. Estrada, K. *et al.* Genome-wide meta-analysis identifies 56 bone mineral density loci and reveals 14 loci associated with risk of fracture. *Nat. Genet.* **44**, 491–501 (2012).
15. ENCODE Project Consortium. An integrated encyclopedia of DNA elements in the human genome. *Nature* **489**, 57–74 (2012).
16. Ward, L.D. & Kellis, M. HaploReg: a resource for exploring chromatin states, conservation, and regulatory motif alterations within sets of genetically linked variants. *Nucleic Acids Res.* **40**, D930–D934 (2012).
17. Rymer, J. & Wildsoet, C.F. The role of the retinal pigment epithelium in eye growth regulation and myopia: a review. *Vis. Neurosci.* **22**, 251–261 (2005).
18. Fernández-Medarde, A. *et al.* RasGRF1 disruption causes retinal photoreception defects and associated transcriptomic alterations. *J. Neurochem.* **110**, 641–652 (2009).
19. Tonini, R. *et al.* Expression of Ras-GRF in the SK-N-BE neuroblastoma accelerates retinoic-acid-induced neuronal differentiation and increases the functional expression of the IRK1 potassium channel. *Eur. J. Neurosci.* **11**, 959–966 (1999).
20. Abd-El-Barr, M.M. *et al.* Genetic dissection of rod and cone pathways in the dark-adapted mouse retina. *J. Neurophysiol.* **102**, 1945–1955 (2009).
21. Beyer, B. *et al.* Absence seizures in C3H/HeJ and knockout mice caused by mutation of the AMPA receptor subunit *Gria4*. *Hum. Mol. Genet.* **17**, 1738–1749 (2008).
22. Connaughton, V. Glutamate and glutamate receptors in the vertebrate retina. In *Webvision: The Organization of the Retina and Visual System* (eds. Kolb, H., Fernandez, E. & Nelson, R.) (Natural Library of Medicine, Salt Lake City, Utah, 1995).
23. Yang, J., Nemargut, J.P. & Wang, G.Y. The roles of ionotropic glutamate receptors along the On and Off signaling pathways in the light-adapted mouse retina. *Brain Res.* **1390**, 70–79 (2011).
24. Smith, E.L. III, Fox, D.A. & Duncan, G.C. Refractive-error changes in kitten eyes produced by chronic on-channel blockade. *Vision Res.* **31**, 833–844 (1991).
25. Fogel, B.L. *et al.* RBFOX1 regulates both splicing and transcriptional networks in human neuronal development. *Hum. Mol. Genet.* **21**, 4171–4186 (2012).
26. Zhang, X., Yang, D. & Hughes, B.A. KCNQ5/K_v7.5 potassium channel expression and subcellular localization in primate retinal pigment epithelium and neural retina. *Am. J. Physiol. Cell Physiol.* **301**, C1017–C1026 (2011).
27. Pattnaik, B.R. & Hughes, B.A. Effects of KCNQ channel modulators on the M-type potassium current in primate retinal pigment epithelium. *Am. J. Physiol. Cell Physiol.* **302**, C821–C833 (2012).
28. Troilo, D., Nickla, D.L., Mertz, J.R. & Summers Rada, J.A. Change in the synthesis rates of ocular retinoic acid and scleral glycosaminoglycan during experimentally altered eye growth in marmosets. *Invest. Ophthalmol. Vis. Sci.* **47**, 1768–1777 (2006).
29. Mertz, J.R. & Wallman, J. Choroidal retinoic acid synthesis: a possible mediator between refractive error and compensatory eye growth. *Exp. Eye Res.* **70**, 519–527 (2000).
30. McFadden, S.A., Howlett, M.H. & Mertz, J.R. Retinoic acid signals the direction of ocular elongation in the guinea pig eye. *Vision Res.* **44**, 643–653 (2004).
31. Parker, R.O. & Crouch, R.K. Retinol dehydrogenases (RDHs) in the visual cycle. *Exp. Eye Res.* **91**, 788–792 (2010).
32. Schéele, S. *et al.* Laminin isoforms in development and disease. *J. Mol. Med. (Berl.)* **85**, 825–836 (2007).
33. Zhang, Y., Liu, Y. & Wildsoet, C.F. Bidirectional, optical sign-dependent regulation of *BMP2* gene expression in chick retinal pigment epithelium. *Invest. Ophthalmol. Vis. Sci.* **53**, 6072–6080 (2012).
34. Ramdas, W.D. *et al.* A genome-wide association study of optic disc parameters. *PLoS Genet.* **6**, e1000978 (2010).
35. Gallardo, M.E. *et al.* Analysis of the developmental *SIX6* homeobox gene in patients with anophthalmia/microphthalmia. *Am. J. Med. Genet. A.* **129A**, 92–94 (2004).
36. Gal, A. *et al.* Autosomal-recessive posterior microphthalmos is caused by mutations in *PRSS56*, a gene encoding a trypsin-like serine protease. *Am. J. Hum. Genet.* **88**, 382–390 (2011).
37. Orr, A. *et al.* Mutations in a novel serine protease *PRSS56* in families with nanophthalmos. *Mol. Vis.* **17**, 1850–1861 (2011).
38. Nair, K.S. *et al.* Alteration of the serine protease *PRSS56* causes angle-closure glaucoma in mice and posterior microphthalmia in humans and mice. *Nat. Genet.* **43**, 579–584 (2011).
39. Rossin, E.J. *et al.* Proteins encoded in genomic regions associated with immune-mediated disease physically interact and suggest underlying biology. *PLoS Genet.* **7**, e1001273 (2011).

Virginie J M Verhoeven^{1,2,68}, Pirro G Hysi^{3,68}, Robert Wojciechowski^{4,5,68}, Qiao Fan^{6,68}, Jeremy A Guggenheim^{7,68}, René Höhn^{8,68}, Stuart MacGregor⁹, Alex W Hewitt^{10,11}, Abhishek Nag³, Ching-Yu Cheng^{6,12,13}, Ekaterina Yonova-Doing³, Xin Zhou⁶, M Kamran Ikram^{6,12,13}, Gabriëlle H S Buitendijk^{1,2}, George McMahon¹⁴, John P Kemp¹⁴, Beate St Pourcain¹⁵, Claire L Simpson⁴, Kari-Matti Mäkelä¹⁶, Terho Lehtimäki¹⁶, Mika Kähönen¹⁷, Andrew D Paterson¹⁸, S Mohsen Hosseini¹⁸, Hoi Suen Wong¹⁸, Liang Xu¹⁹, Jost B Jonas²⁰, Olavi Pärssinen^{21,22,23}, Juho Wedenoja²⁴, Shea Ping Yip²⁵, Daniel W H Ho^{7,26}, Chi Pui Pang²⁶, Li Jia Chen²⁷, Kathryn P Burdon²⁸, Jamie E Craig²⁸, Barbara E K Klein²⁹, Ronald Klein²⁹, Toomas Haller³⁰, Andres Metspalu³⁰, Chiea-Chuen Khor^{6,12,31,32}, E-Shyong Tai^{6,33,34}, Tin Aung^{12,13}, Eranga Vithana¹³, Wan-Ting Tay¹³, Veluchamy A Barathi^{12,13,34}, Consortium for Refractive Error and Myopia (CREAM)³⁵, Peng Chen⁶, Ruoying Li⁶, Jiemin Liao¹², Yingfeng Zheng¹³, Rick T Ong⁶, Angela Döring^{36,37}, The Diabetes Control and Complications Trial/Epidemiology of Diabetes Interventions and Complications (DCCT/EDIC) Research Group³⁵, David M Evans¹⁴, Nicholas J Timpson¹⁴, Annemieke J M H Verkerk³⁸, Thomas Meitinger³⁹, Olli Raitakari^{40,41}, Felicia Hawthorne⁴², Tim D Spector³, Lennart C Karssen², Mario Pirastu⁴³, Federico Murgia⁴³, Wei Ang⁴⁴, Wellcome Trust Case Control Consortium 2 (WTCCC2)³⁵, Aniket Mishra⁹, Grant W Montgomery⁴⁵, Craig E Pennell⁴⁴, Phillippa M Cumberland^{46,47}, Ioana Cotlarciuc⁴⁸, Paul Mitchell⁴⁹, Jie Jin Wang^{10,49}, Maria Schache¹⁰, Sarayut Janmahasathian⁵⁰, Robert P Igo Jr⁵⁰, Jonathan H Lass^{50,51}, Emily Chew⁵², Sudha K Iyengar^{50,51,53}, The Fuchs' Genetics Multi-Center Study Group³⁵, Theo G M F Gorgels⁵⁴, Igor Rudan⁵⁵, Caroline Hayward⁵⁶, Alan F Wright⁵⁶, Ozren Polasek⁵⁷, Zoran Vataavuk⁵⁸, James F Wilson⁵⁵, Brian Fleck⁵⁹, Tanja Zeller⁶⁰, Alireza Mirshahi⁸, Christian Müller⁶⁰, André G Uitterlinden^{2,37,61}, Fernando Rivadeneira^{2,38,61}, Johannes R Vingerling^{1,2}, Albert Hofman^{2,61}, Ben A Oostra⁶², Najaf Amin², Arthur A B Bergen^{54,63,64}, Yik-Ying Teo^{6,65}, Jugnoo S Rahi^{45,47,66}, Veronique Vitart⁵⁶, Cathy Williams¹⁵, Paul N Baird¹⁰, Tien-Yin Wong^{6,12,13}, Konrad Oexle³⁹, Norbert Pfeiffer⁸, David A Mackey^{10,11}, Terri L Young⁴², Cornelia M van Duijn², Seang-Mei Saw^{6,12,13,34,69}, Joan E Bailey-Wilson^{4,69}, Dwight Stambolian^{67,69}, Caroline C Klaver^{1,2,69} & Christopher J Hammond^{3,69}

¹Department of Ophthalmology, Erasmus Medical Center, Rotterdam, The Netherlands. ²Department of Epidemiology, Erasmus Medical Center, Rotterdam, The Netherlands. ³Department of Twin Research and Genetic Epidemiology, King's College London School of Medicine, London, UK. ⁴Inherited Disease Research Branch, National Human Genome Research Institute, US National Institutes of Health, Baltimore, Maryland, USA. ⁵Department of Epidemiology, Johns Hopkins Bloomberg School of Public Health, Baltimore, Maryland, USA. ⁶Saw Swee Hock School of Public Health, National University Health Systems, National University of Singapore, Singapore. ⁷Centre for Myopia Research, School of Optometry, The Hong Kong Polytechnic University, Hong Kong. ⁸Department of Ophthalmology, University Medical Center Mainz, Mainz, Germany. ⁹Department of Statistical Genetics, Queensland Institute of Medical Research, Herston, Brisbane, Queensland, Australia. ¹⁰Centre for Eye Research Australia (CERA), University of Melbourne, Royal Victorian Eye and Ear Hospital, Melbourne, Victoria, Australia. ¹¹Centre for Ophthalmology and Visual Science, Lions Eye Institute, University of Western Australia, Perth, Western Australia, Australia. ¹²Department of Ophthalmology, National University Health Systems, National University of Singapore, Singapore. ¹³Singapore Eye Research Institute, Singapore National Eye Centre, Singapore. ¹⁴Medical Research Council Centre for Causal Analyses in Translational Epidemiology, School of Social and Community Medicine, University of Bristol, Bristol, UK. ¹⁵School of Social and Community Medicine, University of Bristol, Bristol, UK. ¹⁶Department of Clinical Chemistry, Fimlab Laboratories and School of Medicine, University of Tampere, Tampere, Finland. ¹⁷Department of Clinical Physiology, Tampere University Hospital and School of Medicine, University of Tampere, Tampere, Finland. ¹⁸Program in Genetics and Genome Biology, Hospital for Sick Children and University of Toronto, Toronto, Ontario, Canada. ¹⁹Beijing Institute of Ophthalmology, Beijing Tongren Hospital, Capital Medical University, Beijing, China. ²⁰Department of Ophthalmology, Medical Faculty Mannheim, Ruprecht-Karls-University Heidelberg, Mannheim, Germany. ²¹Department of Health Sciences, University of Jyväskylä, Jyväskylä, Finland. ²²Gerontology Research Center, University of Jyväskylä, Jyväskylä, Finland. ²³Department of Ophthalmology, Central Hospital of Central Finland, Jyväskylä, Finland. ²⁴Department of Public Health, Hjelt Institute, University of Helsinki, Helsinki, Finland. ²⁵Department of Health Technology and Informatics, The Hong Kong Polytechnic University, Hong Kong. ²⁶Department of Ophthalmology and Visual Sciences, The Chinese University of Hong Kong, Hong Kong Eye Hospital, Kowloon, Hong Kong. ²⁷Department of Ophthalmology and Visual Sciences, The Chinese University of Hong Kong, Prince of Wales Hospital, Shatin, Hong Kong. ²⁸Department of Ophthalmology, Flinders University, Adelaide, South Australia, Australia. ²⁹Department of Ophthalmology and Visual Sciences, University of Wisconsin School of Medicine and Public Health, Madison, Wisconsin, USA. ³⁰Estonian Genome Center, University of Tartu, Tartu, Estonia. ³¹Department of Pediatrics, National University of Singapore, Singapore. ³²Division of Human Genetics, Genome Institute of Singapore, Singapore. ³³Department of Medicine, National University of Singapore, Singapore. ³⁴Duke-National University of Singapore Graduate Medical School, Singapore. ³⁵A full list of members appears in the **Supplementary Note**. ³⁶Institute of Epidemiology I, Helmholtz Zentrum München-German Research Center for Environmental Health, Neuherberg, Germany. ³⁷Institute of Epidemiology II, Helmholtz Zentrum München-German Research Center for Environmental Health, Neuherberg, Germany. ³⁸Department of Internal Medicine, Erasmus Medical Center, Rotterdam, The Netherlands. ³⁹Institute of Human Genetics, Technical University Munich, Munich, Germany. ⁴⁰Research Centre of Applied and Preventive Medicine, University of Turku, Turku, Finland. ⁴¹Department of Clinical Physiology and Nuclear Medicine, Turku University Hospital, Turku, Finland. ⁴²Department of Pediatric Ophthalmology, Duke Eye Center For Human Genetics, Durham, North Carolina, USA. ⁴³Institute of Population Genetics, National Research Council, Sassari, Italy. ⁴⁴School of Women's and Infants' Health, University of Western Australia, Perth, Western Australia, Australia. ⁴⁵Department of Molecular Epidemiology, Queensland Institute of Medical Research, Herston, Brisbane, Queensland, Australia. ⁴⁶Medical Research Council Centre of Epidemiology for Child Health, Institute of Child Health, University College London, London, UK. ⁴⁷Ulverschroft Vision Research Group, University College London, London, UK. ⁴⁸Imperial College Cerebrovascular Research Unit (ICCRU), Division of Brain Sciences, Department of Medicine, Imperial College London, London, UK. ⁴⁹Department of Ophthalmology, Centre for Vision Research, Westmead Millennium Institute, University of Sydney, Sydney, New South Wales, Australia. ⁵⁰Department of Epidemiology and Biostatistics, Case Western Reserve University, Cleveland, Ohio, USA. ⁵¹Department of Ophthalmology and Visual Sciences, Case Western Reserve University and University Hospitals Eye Institute, Cleveland, Ohio, USA. ⁵²National Eye Institute, US National Institutes of Health, Bethesda, Maryland, USA. ⁵³Department of Genetics, Case Western Reserve University, Cleveland, Ohio, USA. ⁵⁴Department of Clinical and Molecular Ophthalmogenetics, Netherlands Institute of Neurosciences (NIN), an Institute of the Royal Netherlands Academy of Arts and Sciences (KNAW), Amsterdam, The Netherlands. ⁵⁵Centre for Population Health Sciences, University of Edinburgh, Edinburgh, UK. ⁵⁶Medical Research Council Human Genetics Unit, Institute of Genetics and Molecular Medicine, University of Edinburgh, Edinburgh, UK. ⁵⁷Faculty of Medicine, University of Split, Split, Croatia. ⁵⁸Department of Ophthalmology, Sisters of Mercy University Hospital, Zagreb, Croatia. ⁵⁹Princess Alexandra Eye Pavilion, Edinburgh, UK. ⁶⁰Clinic for General and Interventional Cardiology, University Heart Center Hamburg, Hamburg, Germany. ⁶¹Netherlands Consortium for Healthy Ageing, Netherlands Genomics Initiative, The Hague, The Netherlands. ⁶²Department of Clinical Genetics, Erasmus Medical Center, Rotterdam, The Netherlands. ⁶³Department of Clinical Genetics, Academic Medical Center, Amsterdam, The Netherlands. ⁶⁴Department of Ophthalmology, Academic Medical Center, Amsterdam, The Netherlands. ⁶⁵Department of Statistics and Applied Probability, National University of Singapore, Singapore. ⁶⁶Institute of Ophthalmology, Moorfields Eye Hospital, London, UK. ⁶⁷Department of Ophthalmology, University of Pennsylvania, Philadelphia, Pennsylvania, USA. ⁶⁸These authors contributed equally to this work. ⁶⁹These authors jointly directed this work. Correspondence should be addressed to C.C.W.K. (c.c.w.klaver@erasmusmc.nl).

ONLINE METHODS

Study design. We performed a meta-analysis on directly genotyped and imputed SNPs from individuals of European ancestry in 27 studies, with a total of 37,382 individuals. Subsequently, we evaluated significantly associated SNPs in 8,376 subjects of Asian origin from 5 different studies and performed a meta-analysis on all studies combined.

Subjects and phenotyping. All studies participating in this meta-analysis are part of CREAM. All studies had a population-based design and had a similar protocol for phenotyping (**Supplementary Table 1**). Eligible participants underwent a complete ophthalmological examination, including a non-dilated measurement of refractive error for both eyes. Exclusion criteria were all conditions that could alter refraction, such as cataract surgery, laser refractive procedures, retinal detachment surgery, keratoconus or ocular or systemic syndromes. Inclusion criteria included age of 25 years and over and data on refractive error and genotype.

The meta-analysis of stage 1 was based on 27 studies of European ancestry: 1958 British Birth Cohort, ALSPAC, ANZRAG, AREDS1a1b, AREDS1c, CROATIA-Korcula, CROATIA-Split, CROATIA-Vis, EGCUT, FECD, TEST/BATS, FITSA, Framingham, GHS 1, GHS 2, KORA, ORCADES, TwinsUK, WESDR, YFS, ERF, DCCT, BMES, RS1, RS2, RS3 and OGP Talana. Stage 2 comprised 5 Asian studies: Beijing Eye Study, SCES, SIMES, SINDI and SP2.

Information on general methods, demographics and phenotyping and genotyping methods of the study cohorts can be found in **Supplementary Table 1** and the **Supplementary Note**. All studies were performed with the approval of their local medical ethics committee, and written informed consent was obtained from all participants in accordance with the Declaration of Helsinki.

Genotyping and imputation. Information on genotyping in each cohort, the particular platforms used to perform genotyping and the methods of imputation can be found in more detail in **Supplementary Table 5**. To produce consistent data sets and enable meta-analysis of studies across different genotyping platforms, the studies performed genomic imputation on available HapMap Phase 2 genotypes with MACH⁴⁰ or IMPUTE⁴¹, using the appropriate ancestry groups as templates.

Each study applied stringent quality control procedures before imputation, including MAF cutoffs, Hardy-Weinberg equilibrium ($P > 1 \times 10^{-7}$), genotypic success rate (>95%), mendelian inconsistencies, exclusion of individuals with more than 5% shared ancestry (exception made for family-based cohorts in which due adjustment for family relationship was made) and removal of all individuals whose ancestry as determined through genetic analysis did not match the prevailing ancestry group of the corresponding cohort. SNPs with low imputation quality were filtered using metrics specific to the imputation method and thresholds used in previous GWAS analyses. Hence, imputation quality criteria varied slightly between studies, and low-confidence imputed SNPs were omitted in the meta-analysis for individual studies.

Statistical analysis. Spherical equivalent was calculated according to the standard formula ($SE = \text{sphere} + 1/2 \text{ cylinder}$), and the mean value from two eyes was used for analysis. When data from only one eye was available, the spherical equivalent of this eye was used.

Each cohort performed association analyses in which the spherical equivalent was the dependent variable and genotypes (number of alleles in each of the HapMap 2 loci) were the independent variables. Analyses in all cases also adjusted for sex and age at the time of phenotype measurement. In family-based cohorts, a score test-based association test was used to adjust for within-family relatedness (**Supplementary Note**)^{42,43}. Study-specific λ estimates are shown in **Supplementary Table 2**.

All study effect estimates were corrected using genomic control and were oriented to the positive strand of the NCBI Build 36 reference sequence of the human genome, which was the genomic build on which most available genotyping platforms were based. Coordinates and further annotations for the SNPs were converted into Build 37, the most recent version of the available builds at the time of writing.

Meta-analyses used effect size estimations (β regression coefficients) and standard errors from individual cohorts' summary statistics. Random effects were assumed for all the meta-analyses that were performed using GWAMA⁴⁴.

We tested for heterogeneous effects between the two ancestry groups using METAL⁴⁵ for Linux. For the purpose of these analyses, we defined significance as equal to or better than the conventional multiple-testing genome-wide thresholds of association ($P < 5.0 \times 10^{-8}$) for stage 1 and nominally significant probabilities ($P < 0.05$) for stage 2. Manhattan, regional and forest plots were made using R (see URLs) and LocusZoom (see URLs)⁴⁶.

For the Rotterdam Study 1–3, a weighted genetic risk score per individual was calculated using the regression coefficients from the GWAS meta-analysis model for the association of SNPs within the associated 26 loci (**Tables 1** and **2**; for each locus, only one SNP was included in the analysis) and the individual allele dosages per genotype to evaluate the relationships between myopia ($SE \leq -3 D$), emmetropia ($-1.5 D \leq SE \leq 1.5 D$) and hyperopia ($SE \geq 3 D$). The weighted risk scores were categorized, and mean ORs per risk score category were calculated for subjects with myopia versus hyperopia, using the middle risk score category as a reference. Subsequently, AUCs were calculated for myopia versus emmetropia and myopia versus hyperopia. Lastly, the proportion of variance of spherical equivalent explained by the identified SNPs was calculated. For these analyses, we used SPSS version 20.0.0.

Gene expression data in human eye tissue. Independently designed, collected and reported human ocular tissue array data from two different sources, as well as literature reviews, were used to verify evidence of expression of the candidate genes.

RPE, photoreceptors and choroid. Human gene expression data for RPE, photoreceptors and choroid were obtained essentially as described⁴⁷, and the data set has been deposited in NCBI's Gene Expression Omnibus⁴⁸ (accession GSE20191). In short, postmortem eye bulbs (RPE was obtained from six donor eyes, choroid was obtained from three donor eyes and photoreceptors were obtained from three donor eyes), provided by the Corneabank Amsterdam, were rapidly frozen using liquid nitrogen. Donors were between 63 and 78 years old and had no known history of eye pathology. Cryosections were cut from the macula, and histology was used to confirm a normal histological appearance. RPE, photoreceptor and choroidal cells were isolated from macular sections using the Laser Microdissection System (PALM). Total RNA was isolated, and the mRNA component was amplified, labeled and hybridized to a 44K microarray (Agilent Technologies)⁴⁹. At least three to six microarrays were performed per tissue. Sample isolation, procedures and expression microarray analysis were carried out according to MIAMI guidelines. To bring order in the level of expression, we sorted all the genes represented on the 44K microarray by increasing expression, and we calculated the corresponding percentiles (**Supplementary Table 3a**).

Sclera, cornea and optic nerve. We assessed expression of the associated genes in sclera, cornea and optic nerve tissue in an additional data set (data not shown). Adult eyes were obtained from the North Carolina Eye Bank (Winston-Salem, North Carolina). All whole globes were immersed in RNALater (Qiagen) within 6.5 h of collection, shipped overnight on ice and dissected on the day of arrival. The retina, choroid and sclera tissues were isolated at the posterior pole using a circular, double-embedded technique using round 7-mm and 5-mm biopsy punches. To reduce contamination of the retina to the other ocular tissue samples, the second biopsy punch of 5 mm was used in the center of the 7-mm punch after retinal removal. RNA samples (with quality control of RNA concentration and 260/280 nm ratios performed using Nanodrop; Invitrogen) were hybridized to whole-genome microarray Illumina HumanHT-12 v4 Expression BeadChips (with over 25,000 genes and 48,000 probes) in 2 batches. The first batch was hybridized to adult RPE, choroid and sclera RNA samples ($n = 6$). The second batch of newer chips with additional probes was hybridized to adult optic nerve and cornea samples ($n = 6$). The data were exported from Illumina GenomeStudio and were \log_2 transformed. Sample outliers were determined by principal-component analyses using the Hotelling's T2 test⁵⁰ (at 95% confidence interval) and removed from further analyses. Data intensity was normalized by quantile normalization followed by multichip averaging⁵¹ to reduce chip effects. For each tissue type, the probes with signal intensities below background levels and those with the lowest (5%) signal intensities (detection $P < 0.10$) were excluded. Evidence of expression for the remaining probes was defined by detection $P < 0.05$. Probes with detection $P < 0.10$ or > 0.05 required additional tissue expression support from EyeSAGE or literature reports (**Supplementary Table 3b**).

Search for regulatory elements. We used the 'Integrated Regulation from ENCODE' track in the UCSC Genome Browser to look at H3K27ac modification as a mark of active regulatory elements. Numbers of H3K27ac modifications were counted between the associated top SNP from a locus and the nearest gene and within the nearest gene itself. We also used HaploReg¹⁶ annotations to look for other signs of regulatory activity at the site of the associated SNP itself, such as enhancer histone marks, DNase hypersensitivity sites, binding proteins and motifs changed.

Pathway analyses. We used two different programs for pathway analysis: Ingenuity (see URLs), version August 2012, application build 172788, content version 14197757) and the Disease Association Protein-Protein Link Evaluator (DAPPLE)³⁹.

Subcellular localization assignment and functional annotation of myopia-associated disease genes as well as molecular pathway analysis were carried out using the Ingenuity knowledge database (IPA). The candidate myopia-causing genes discovered in this study were entered into IPA. We used the 'IPA toggle subcellular layout' function to show the subcellular location (extracellular, plasma membrane, cytoplasm, nucleus or unknown) of the proteins corresponding to these genes, yielding a first glance at which signaling molecules and pathways are involved in myopia. Subsequently, we used the IPA 'connect' function to discover potential direct or indirect functional relationships or molecular pathways in between these entries. This yielded unexpectedly few hits, which suggests molecular disease heterogeneity and/or functional redundancy in the pathobiological events leading to myopia. Next, we used the IPA 'overlay' function to annotate the myopia candidate genes with their involvement in 'functions and diseases', 'canonical pathways' and a range of custom-made gene lists from previous studies, including

photoreceptor-, RPE- and choroid-specific transcripts (ref. 52 and data not shown). Lastly, we used DAPPLE³⁹ to look for physical connections between proteins encoded by disease-related genes from associated regions.

40. Li, Y., Willer, C.J., Ding, J., Scheet, P. & Abecasis, G.R. MaCH: using sequence and genotype data to estimate haplotypes and unobserved genotypes. *Genet. Epidemiol.* **34**, 816–834 (2010).
41. Marchini, J., Howie, B., Myers, S., McVean, G. & Donnelly, P. A new multipoint method for genome-wide association studies by imputation of genotypes. *Nat. Genet.* **39**, 906–913 (2007).
42. Aulchenko, Y.S., Struchalin, M.V. & van Duijn, C.M. ProbABEL package for genome-wide association analysis of imputed data. *BMC Bioinformatics* **11**, 134 (2010).
43. Chen, W.M. & Abecasis, G.R. Family-based association tests for genomewide association scans. *Am. J. Hum. Genet.* **81**, 913–926 (2007).
44. Mägi, R. & Morris, A.P. GWAMA: software for genome-wide association meta-analysis. *BMC Bioinformatics* **11**, 288 (2010).
45. Willer, C.J., Li, Y. & Abecasis, G.R. METAL: fast and efficient meta-analysis of genomewide association scans. *Bioinformatics* **26**, 2190–2191 (2010).
46. Pruim, R.J. *et al.* LocusZoom: regional visualization of genome-wide association scan results. *Bioinformatics* **26**, 2336–2337 (2010).
47. Booi, J.C. *et al.* Functional annotation of the human retinal pigment epithelium transcriptome. *BMC Genomics* **10**, 164 (2009).
48. Edgar, R., Domrachev, M. & Lash, A.E. Gene Expression Omnibus: NCBI gene expression and hybridization array data repository. *Nucleic Acids Res.* **30**, 207–210 (2002).
49. van Soest, S.S. *et al.* Comparison of human retinal pigment epithelium gene expression in macula and periphery highlights potential topographic differences in Bruch's membrane. *Mol. Vis.* **13**, 1608–1617 (2007).
50. Hotelling, H. The generalization of Student's ratio. *Ann. Math. Stat.* **2**, 360–378 (1931).
51. Irizarry, R.A. *et al.* Exploration, normalization, and summaries of high density oligonucleotide array probe level data. *Biostatistics* **4**, 249–264 (2003).
52. Booi, J.C. *et al.* A new strategy to identify and annotate human RPE-specific gene expression. *PLoS One* **5**, e9341 (2010).